

SciEn Conference Series: Engineering Vol. 3, 2025, pp 337-342

https://doi.org/10.38032/scse.2025.3.95

Numerical Comparison of Natural Convection Heat Transfer in Air- and Water-Filled Enclosures

Tanvir Ahmed Fahim, Md. Mahbubur Rahman, Inkiad Haque Sharar*

Department of Mechanical Engineering, Khulna University of Engineering & Technology, Khulna-9203, Bangladesh

ABSTRACT

This study investigates the natural convection heat transfer in a C-shaped enclosure filled with air and water through numerical simulation. The enclosure with varying aspect ratios (the ratio of outer length to inner length of the enclosure) is considered to examine the effects of both enclosure shape and fluid properties on heat transfer rate. The outer C-shaped boundary is set to a higher temperature compared to the inner one, while the connecting walls between the hot wall and cold rib are treated as adiabatic. The numerical analysis is conducted in ANSYS Fluent 20.2 assuming a 2-D problem setup at the Rayleigh number ranging from 10⁴ to 10⁶, capturing the behavior of both fluids under low to moderate buoyancy-driven flow conditions. Streamline and temperature contour visualizations in the result analysis reveal the formation of primary and secondary eddies, with central, large eddies dominating the enclosure and smaller eddies forming in the gap between the cold rib and hot wall. These secondary eddies promote mixing and enhance convective currents by disrupting the primary flow. This leads to increased circulation within the enclosure, thereby raising the heat transfer. Water-filled enclosures predominantly exhibit higher heat transfer than air-filled enclosures due to water's superior thermal conductivity and heat capacity, which facilitate more intense convective eddy circulation. However, the eddy dynamics in air-filled enclosures can become especially favorable for transferring heat, even in comparison to water-filled counterparts This work underscores the role of enclosure shape and fluid properties in enhancing convective heat transfer, providing insights for optimizing thermal management in confined geometries.

Keywords: Rayleigh Number, Air, Water, Nusselt Number, Natural Convection.



Copyright @ All authors

This work is licensed under a Creative Commons Attribution 4.0 International License.

1. Introduction

convection occurs in fluids when Natural differences in density, driven by temperature variations, cause fluid movement without external forces. This process, governed by buoyancy, happens as fluid near a heat source absorbs heat, expands, becomes less dense, and rises, while cooler, denser fluid sinks [1]. Recently, natural convection has drawn significant research interest for its applications in fields like geophysics, geothermal systems, building insulation, and industrial separation processes. Studies focus on thermal behavior and fluid flow in various enclosures and boundary conditions using air, water, and other fluids. Since standard cavities cannot fully describe natural convection in complex environments, researchers are exploring a range of enclosure shapes—including square [2], trapezoidal [3], Cshaped [4], L-shaped [5], U-shaped [6], T-shaped [7] and Vshaped [8]—to better capture and analyze these physical phenomena

Inam [2] investigated the effects of varying inclination angles on the convective behavior of natural convection and discovered that convective heat transfer improves as the inclination angle increases. Mahmud et al. [3] noted that raising the inclination angle of the trapezoidal enclosure improves the convective heat exchange for both geometries, with the trapezoidal cavity demonstrating a greater impact than the square enclosure. Makulati et al [4] used water-alumina nanofluid in an inclined C-shaped enclosure with varying aspect ratio, Rayleigh number, and inclination angle and found minimum Nusselt number took

place at an aspect ratio 0.2 and inclination angle of 45°. Mahmoodi [5] studied L-shaped cavities filled with Cu nanoparticles with various aspect ratios, the volume fraction of nanofluid, and Rayleigh number where he found that heat transfer rate increases with decreasing aspect ratio. Yıldız et al. [6] investigated the natural convection of nanofluids within a U-shaped enclosure, specifically analyzing the impact of cold rib dimensions on heat transfer performance. The research demonstrated that varying rib sizes significantly influenced thermal efficiency, highlighting their crucial role in optimizing heat transfer in thermal management applications. A study of inclined T-shaped cavities was done by Rouijja et al [7] for varying inclination angles and Rayleigh numbers and observed Nusselt number and mass flow rate decreases with increasing inclination angle. Bhowmick et al [8] studied the V-shaped enclosure filled with water with a certain Prandtl number=0.7, various Rayleigh numbers, and aspect ratios.

It is discernible from the preceding literature review that the research on investigating natural convection heat transfer on different enclosures with different working fluids such as air [9], water [10-11], and nanofluids [4-6] are available in the literature. Although there is a comparison research work on air and water in rectangular enclosures [12], the comparison of heat transfer behavior between air and water in C-shaped enclosures has not yet been explored. In this numerical comparison study, several simulations are performed investigating natural convection heat transfer in air and water-filled C-shaped enclosures the aspect ratios

AR=0.3,0.5,0.7 at Rayleigh numbers Ra = 10⁴, 10⁵, 10⁶ using ANSYS Fluent 20.2. Streamlines and isotherm contours are analyzed for different geometries. This paper is organized as follows section 1 provides a general introduction to natural convection phenomena with a literature review on heat transfer in various geometries and working fluids and research gap. Section 2 provides methodology incorporating problem statement, governing equation, geometry and meshing, validation under numerical simulation. Section 3 outlines numerical results comparison for natural convection of air and water in a C-shaped enclosure and analytical discussion. Finally, conclusions are drawn in Section 4.

2. Numerical simulation

2.1 Problem statement

This investigation examines a C-shaped enclosure with the dimensions depicted in Fig. 1. The setup includes an outer C-shaped geometry H and an inner L, along with two walls that connect these two shapes. The outer C-shaped geometry is designated as hot surfaces at a temperature T_H , while the inner geometry is considered to have cold surfaces at a temperature T_C (where $T_H \!\!>\!\! T_C$). The two connecting walls are assumed to be adiabatic for the scope of this research. The aspect ratio of this configuration is expressed as the ratio of the inner C-shaped edge dimensions to the outer C-shaped edge dimensions, hence, AR=L/H

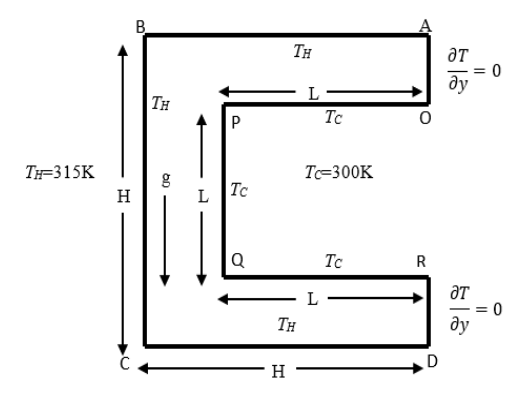


Fig. 1: Schematic diagram of the C-shaped enclosure.

The fluid flow is simulated as two-dimensional phenomena with the assumptions [9] (a) fluids are Newtonian, incompressible, and laminar flow (b) Boussinesq approximation is invoked and (c)radiation effects are neglected. **Table 1** shows the thermophysical properties of Air and Water at 300K.

Table 1 : Thermophysical properties of Air & Water[1].

Properties	Air	Water
$C_p(j/kg k)$	1004.71	4181.37
$\rho(\mathrm{kg}/m^3)$	1.16	996.51
k (w/m k)	0.0268	0.6103
$\beta(K^{-1})$	0.003252	0.003252

2.2 Numerical approach and governing equations:

The following governing equations—continuity, momentum, and energy—as well as boundary conditions utilizing the Boussinesq approximation control the solution of the natural convection flows inside the C-shaped enclosure. [13].

$$\frac{\partial u}{\partial x} + \frac{\partial v}{\partial x} = 0 \tag{1}$$

$$u\frac{\partial u}{\partial x} + v\frac{\partial u}{\partial x} = \frac{1}{\rho} - \frac{\partial P}{\partial x} + (\frac{\partial^2 u}{\partial x^2} + \frac{\partial^2 u}{\partial y^2})$$
 (2)

$$u\frac{\partial v}{\partial x} + v\frac{\partial v}{\partial y} = \frac{1}{\rho}\frac{\partial P}{\partial y} + \left(\frac{\partial^2 v}{\partial x^2} + \frac{\partial^2 v}{\partial y^2}\right) + g\beta + (T - T_0) \tag{3}$$

$$u\frac{\partial T}{\partial x} + v\frac{\partial T}{\partial x} = k\left(\frac{\partial^2 T}{\partial x^2} + \frac{\partial^2 T}{\partial x^2}\right) \tag{4}$$

Here, ρ stands for air density, k for heat conductivity, and u and v for velocity components in the x and y axes, respectively. β represents the volumetric thermal expansion coefficient, while g represents the acceleration caused by gravity. The equations (Eq. (1) to Eq. (4)) are solved numerically using the finite volume method. The boundary conditions those are set for the problem are:

For left wall: u=v=0; $T_H=315K$ For right wall: u=v=0; $T_c=300K$

For lower and upper walls: u = v = 0; $\frac{\partial T}{\partial y} = 0$

The Rayleigh number defined by Eq. (5) is a dimensionless quantity that indicates the instability of a fluid layer caused by temperature and density variations between its upper and lower surfaces.

$$Ra = \frac{g\beta\rho^2 C_p \Delta T L^3}{\mu k} \tag{(5)}$$

2.3 Geometry and meshing:

ANSYS Fluent 20.2 is used to solve the problem geometry in Fig. 2(a), with convergence conditions for the continuity, x-, y-, and energy equations set to 10–6. After using standard initialization, calculations are carried out until convergence. 120,000 elements are produced by employing the grid size approach with an element size of 0.5mm x 0.5 mm. In Fig. 2(b), the meshing is displayed.

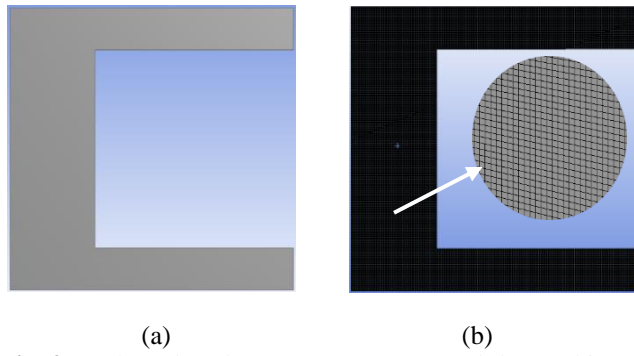


Fig. 2: C-shaped enclosure (a) Geometry and (b) Meshing

A mesh independence test, conducted for a C-shaped enclosure with an aspect ratio of 0.5, two Rayleigh numbers (10⁵), and air as the working fluid, indicated the optimal mesh lies between 50,000 and 150,000 elements, as shown in Fig. 3. Therefore, 120,000 elements were selected for this study.

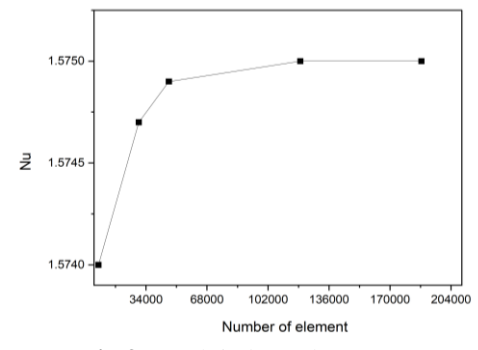


Fig.3: Mesh independency test

2.4 Validation:

The current model has been validated using results from several literature sources, as presented in Table 2. For validation purposes, a 200x200 mm square cavity filled with air was used, featuring one hot wall, one cold wall, and two adiabatic walls. The table shows the Nusselt numbers obtained from both the literature and this study across various Rayleigh numbers, ranging from 10³ to 106 under low to moderate buoyancy-driven flow conditions in the laminar flow regime. Given that the discrepancy between the Nusselt numbers from the literature and those from this study approaches zero at different Rayleigh numbers, the model can be confirmed as valid.

Table 2: Comparison of the Nusselt number at the hot wall of the square cavity against findings from earlier studies

Rayleigh Number	Present study	Khanafer et al [14]	Lai and Yang[15]	Kobra et al [16]
10^{4}	2.247	2.243	2.252	2.2448
10^{5}	4.534	4.519	4.514	4.5216
10 ⁶	8.855	8.799	8.752	8.8262

3. Numerical results and discussion

Three distinct aspect ratios—0.3, 0.5, and 0.7—with Rayleigh numbers ranging from 10⁴ to 10⁶ are the subjects of the results presented here. As the most of the studies does not provide the odd aspect ratios, we used these ratios. Water and air are employed as two distinct fluids. Figures 4 through 12 display the results as a temperature contour and streamline inside the enclosure.

The effects of increasing AR on the flow pattern and temperature distribution inside the enclosure filled with air (a) and water (b) $Ra=10^4$ are shown in Figures 4, 7, and 10. For smaller Rayleigh numbers for different aspect ratios, the streamline's generated eddy often remains centralized. For both air-filled and water-filled enclosures, a primary eddy is formed near the left side of the enclosure and a secondary eddy is formed beneath the cold rib when AR=0.3.

As the aspect ratio increases the number of secondary eddies increases under the cold rib in both water and air -filled enclosure. For AR=0.5, two secondary eddies, and for AR=0.7, multiple secondary eddies are created under the cold rib for both air and water-filled enclosures. For lower Rayleigh numbers the temperature contours seem to remain uniform, especially near the cold rib.

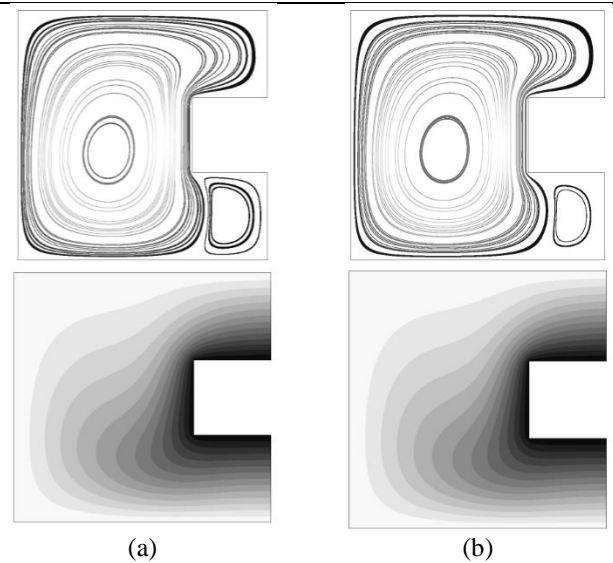


Fig 4. Streamline(up) and Temperature Contour (down) of (a) Air and (b)Water (For AR=0.3 and Ra=10⁴)

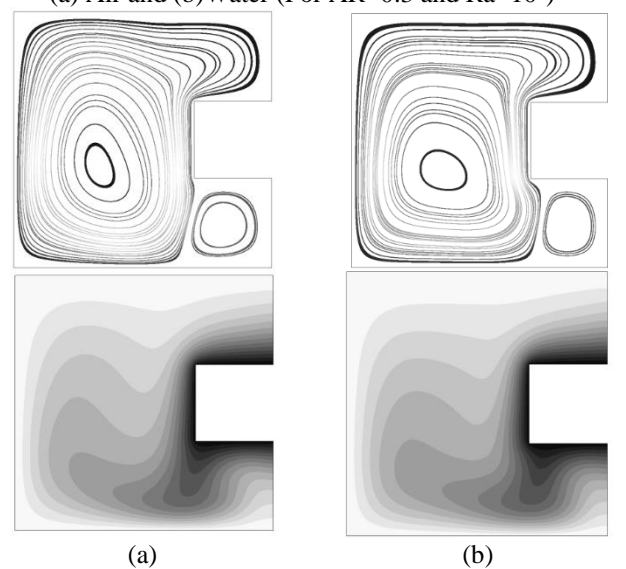


Fig 5. Streamline(up) and Temperature Contour (down) of(a) Air and (b)Water (For AR=0.3 and Ra=10⁵)

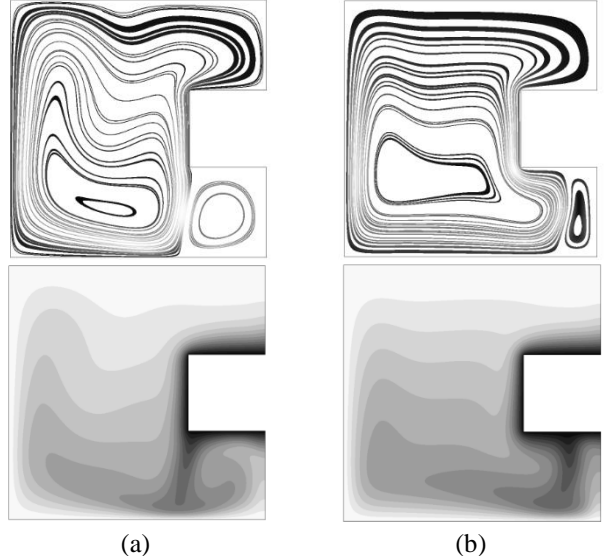


Fig 6. Streamline(up) and Temperature Contour (down) of (a) Air and (b)Water (For AR=0.3 and Ra=10⁶)

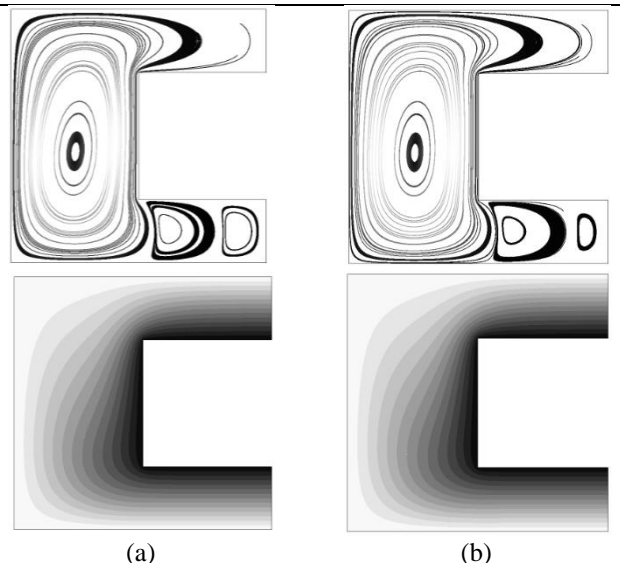


Fig 7. Streamline(up) and Temperature Contour (down) of (a) Air and (b)Water (For AR=0.5 and Ra=10⁴)

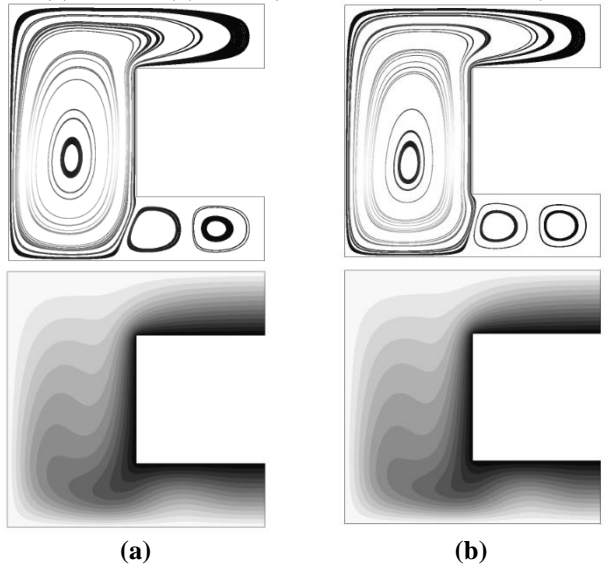


Fig 8. Streamline(up) and Temperature Contour (down) of (a) Air and (b)Water (For AR=0.5 and Ra=10⁵)

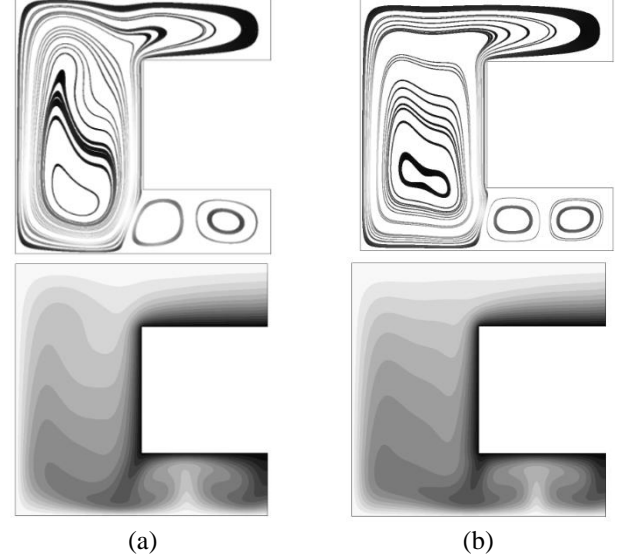


Fig 9. Streamline(up) and Temperature Contour (down) of (a) Air and (b)Water (For AR=0.5 and Ra=10⁶)

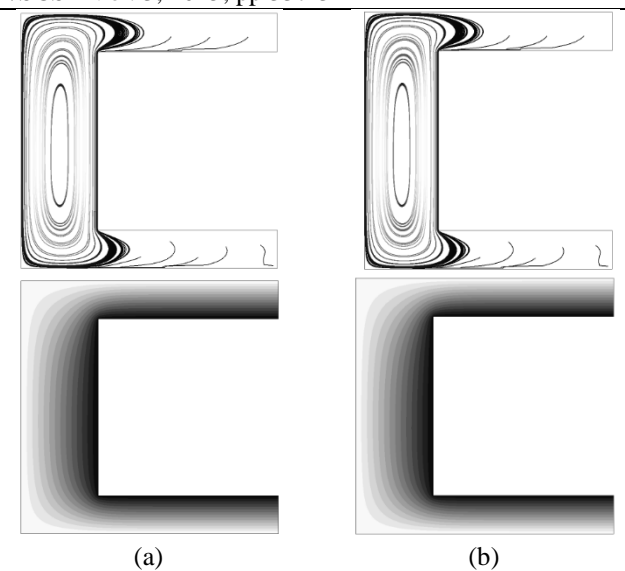


Fig 10. Streamline(up) and Temperature Contour (down) of (a) Air and (b)Water (For AR=0.7 and Ra=10⁴)

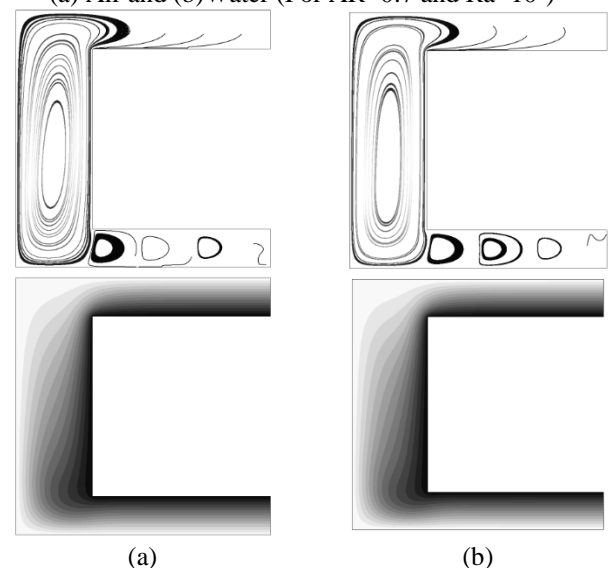


Fig 11. Streamline(up) and Temperature Contour (down) of (a) Air and (b)Water (For AR=0.7 and Ra=10⁵)

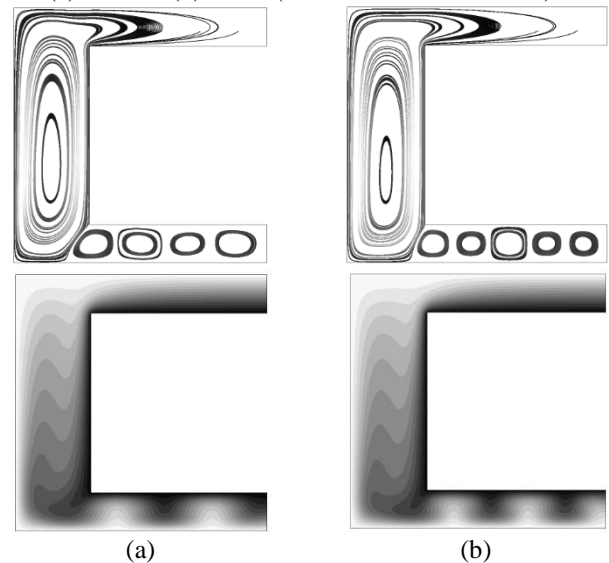


Fig 12. Streamline(up) and Temperature Contour (down) of (a) Air and (b)Water (For AR=0.7 and Ra=10⁶)

From the findings above it can be observed that the temperature contour seems more uniform as the aspect ratio increases at $Ra=10^4$.

Fig 5, Fig 8 and Fig 11 showcase the change in streamline and temperature control with changing aspect ratio both inside air-filled and water-filled enclosure. For a particular aspect ratio water and air both have almost similar type of temperature contours and similar type of boundary layers.

But at Ra=10⁵ as the aspect ratio increases, we see that the thermal boundary layer starts to decrease along the cold rib and becomes more and more uniform. Quite the different scenario from the other cases. In case of streamlines, more and more secondary eddies are formed as the aspect ratio increases as we can see at Ra=10⁵ for AR=0.3. Only one secondary eddy is seen for both air and water but for AR=0.5 it increases to two and finally for AR=0.7 multiple eddies are formed. We see a slightly different pattern in forming eddies in air and water in all the cases.

The fluid is heated by the hot walls and expands as it rises, as shown by the streamline of Fig. 6 at Ra=10⁶ for AR=0.3. The cold rib then cools the fluid, which is then squeezed as it descends. A primary eddy that rotates clockwise is therefore created. Two counter-rotating eddies are formed as the eddy splits. The smaller counterclockwise eddy is situated beneath the cold rib, while the larger clockwise eddy is situated on the left side of the enclosure. This phenomenon occurs for both air and water-filled enclosure. From Fig 9 for AR=0.5 at Ra=106 two secondary eddies are formed in the cases of both water and air. Fig 12 shows that for AR=0.7 at Ra=10⁶ multiple secondary eddies are formed. We can see in the figure that for an air-filled enclosure four secondary eddies are formed while in the case water-filled enclosure five secondary counterclockwise eddies are formed. It signifies the pattern of forming more secondary eddies as the Aspect Ratio increases for a specific Rayleigh Number and it can change at different rates for water and air. Temperature contours show that fluid density near the hot wall decreases and the fluid becomes lighter consequently going upwards. Likewise, fluid density near the cold rib increases accordingly making the fluid heavier and contributing to the cooling effect. As a result, areas near the upper wall show higher temperatures than the areas near the lower wall. Gravitational acceleration plays an important role in this regard. From Fig 6 at Ra=106 for AR=0.3 we can see the effects of gravitational acceleration for (a) air and (b) water more specifically as air is lighter than water gravitational pull works more in air than water. As a result, the temperature of the upper wall and lower wall changes differently in the case of water and air. The thermal boundary layer formed in the air-filled enclosure is less than the thermal boundary layer formed in the water-filled enclosure near the cold rib. From Fig 9 at Ra=10⁶ for AR=0.5 distinct thermal boundary layers are formed at the vicinity of all isothermal walls with the exception of the top wall and secondary eddies are formed. Fig 12 illustrates more distinct thermal boundary layers for AR=0.7 and more secondary eddies are formed. A greater number of secondary eddies are formed in the water than in the air. Therefore, with more eddies forming more distinctive thermal boundary layers are seen as the aspect ratio increases.

4. Conclusions

This study numerically analyzed natural convection heat transfer in C-shaped enclosures filled with air and water,

focusing on the impact of Rayleigh number (Ra), aspect ratio (AR), and fluid type. Key findings include:

- Higher AR values promote secondary eddies, enhancing mixing and convective currents.
- Increased circulation within the enclosure boosts overall heat transfer.
- Water-filled enclosures exhibit superior heat transfer compared to air-filled ones, attributed to water's higher thermal conductivity and heat capacity.
- Water sustains larger, more robust eddies, facilitating efficient heat transport.
- At Ra = 10⁴ and 10⁶ with AR = 0.7, air-filled enclosures demonstrated enhanced convective heat transfer, rivaling water-filled systems under these specific conditions.
- Water generally yields higher Nu values than air, reflecting its improved thermal performance.

References

- [1] Cengel, Y. A., Ghajar, A. J., and Kanoglu, M., Heat and mass transfer: fundamentals and applications, McGraw-Hill Professional, Ed. 5, 2014.
- [2] Inam, M. I., "Direct Numerical Simulation of Laminar Natural Convection in a Square Cavity at Different Inclination Angle," Journal of Engineering Advancements, vol. 01(01), pp. 23-27, 2020.
- [3] Mahmud, M. I., Rahman, M. I., and Liton, M. N. Z., "Numerical Analysis of Laminar Natural Convection Inside Enclosed Squared and Trapezoidal Cavities at Different Inclination Angles," Journal of Engineering Advancements, pp. 1-8, 2024.
- [4] Makulati, N., Kasaeipoor, A., and Rashidi, M., "Numerical study of natural convection of a water—alumina nanofluid in inclined C-shaped enclosures under the effect of magnetic field," *Advanced Powder Technology*, vol. 27, no. 2, pp. 661-672, 2016.
- [5] Mahmoodi, M., "Numerical simulation of free convection of a nanofluid in L-shaped cavities," *International Journal of Thermal Sciences*, vol. 50, no. 9, pp. 1731-1740, 2011
- [6] Yıldız, Ç., Arıcı, M., Karabay, H. and Bennacer, R., "Natural convection of nanofluid in a U-shaped enclosure emphasizing on the effect of cold rib dimensions". *Journal of Thermal Analysis and Calorimetry*, 146, pp.801-811., 2021
- [7] H. Rouijaa, M. El Alami, E. A. Semma, and M. Najam, "Natural convection in an inclined T-shaped cavity," 2011
- .[8] Bhowmick, S., Xu, F., Molla, M. M., and Saha, S. C., "Chaotic phenomena of natural convection for water in a V-shaped enclosure," International Journal of Thermal Sciences, vol. 176, p. 107526, 2022
- [9] Campo, A., and Hasnain, M, "Turbulent natural convection in an air-filled isosceles triangular enclosure". International Journal of Heat and Fluid Flow, 27(3), pp.476-489, 2006.
- [10] Tong, W., and Koster, J. N., "Natural convection of water in a rectangular cavity including density inversion," International journal of heat and fluid flow, vol. 14, no. 4, pp. 366-375, 1993
- [11] Husain, S, and Siddiqui, M. A, "Experimental and numerical analysis of transient natural convection of

- water in a high aspect ratio narrow vertical annulus." Progress in Nuclear Energy 106:1-10,2018
- [12] Khan, J. A., and Guang-Fa, Y. "Comparison of natural convection of water and air in a partitioned rectangular enclosure". International journal of heat and mass transfer, 36(12), 3107-3117. 1993
- [13] Mahmoodi, M. and Hashemi, S. M., "Numerical study of natural convection of a nanofluid in C-shaped enclosures," International Journal of Thermal Sciences, vol. 55, pp. 76-89, 2012.
- [14] Khanafer, K., Vafai, K., and Lightstone, M., "Buoyancy-driven heat transfer enhancement in a two-dimensional enclosure utilizing nanofluids," *International journal of heat and mass transfer*, vol. 46, no. 19, pp. 3639-3653, 2003.
- [15] Lai, F.-H., and Yang, Y.-T., "Lattice Boltzmann simulation of natural convection heat transfer of Al2O3/water nanofluids in a square enclosure," International Journal of Thermal Sciences, vol. 50, no. 10, pp. 1930-1941, 2011

[16] Kobra, F., Quddus, N., and Alim, M. A., "Heat transfer enhancement of Cu-water nanofluid filled in a square cavity with a circular disk under a magnetic field," Procedia Engineering, vol. 90, pp. 582-587, 2014.

NOMENCLATURE

- AR: Aspect ratio of the enclosure
- T: Dimensional Temperature, K
- Ra: Rayleigh number
- k: Thermal conductivity, W/m-K
- u, v: Dimensional velocity components in x and y directions, m/s
 - G: Gravitational acceleration, m/s²
- Nu: Nusselt number
 - g: Acceleration of gravity, m²/s
 - P: Density, kg/m³
- β : Volumetric thermal expansion coefficient, 1/K
- H: Hot
- C: Cold